Iran University of Science and Technology

International Journal of

Railway Research

ISSN: 2423-3838

Fatigue limit state based on alarm thresholds for rail with machine learning

Seyed Mohammad Sadegh Lajevardi[1], Fereidoon Moghadas Nejad[2*], Mehdi Ravanshadnia[3]

[1] Department of Civil Engineering, Science and Research Branch, Islamic Azad University, Tehran, Iran

[2] Department of Civil and Environmental Engineering, Amirkabir University of Technology, Tehran, Iran

[3] Department of Civil Engineering, Science and Research Branch, Islamic Azad University, Tehran, Iran

ARTICLE INFO

Article history:

Received: 08.18.2023

Accepted: 12.25.2023

Published: 12.30.2023

Keywords:

Quality

Alarm threshold

Monitoring

Image processing

Automatic measurement

A B S T R A C T

Public infrastructure is often monitored to assess quality. Alarm thresholds indicate when actions are necessary to improve passenger convenience and operational safety. Based on safety assessments, urgent rail replacements are proposed with a new approach for physical damage threshold extraction. Railway tracks are crucial in transportation, and physical damage can greatly affect their efficiency. During regular visual inspections, inspectors can identify physical damages such as head checks or fatigue cracks. However, there are no definite thresholds to determine the severity of the damages except for rail profile deformation known as wear, which is based on references and standards. Therefore, during the survey and inspection, it is essential to establish alarm thresholds based on limit states for each case. Defects detected before the ultimate limit state can lead to a reduction in quality, which affects the convenience of travel but is not harmful to serviceability. Structure quality control methods use both qualitative and quantitative approaches to assess these cases. However, quantitative assessment reduces the probability of human errors and subjective judgments by inspectors when compared to qualitative assessment. To begin with, image processing is a quantitative tool used to detect defects on rail surfaces. However, the determination of the threshold has been neglected, leading to a lack of anticipation of rail physical damages' lifetime and cost estimation. Therefore, machine learning tools evaluate the output of image processing based on the proposed threshold, which has been expressed in this research. In order to ensure safety, contingency actions will be taken when needed based on the predetermined alarm thresholds.

1. Introduction

In the 1970s, modern limit state design principles were introduced after the allowable stress design (ASD), which includes ultimate limit state (ULS) and serviceability limit state (SLS) designs [1]. As a result, designers must consider two types of limit states in terms of quality and safety when calculating structural designs.

The SLS is a design to certify that a structure is not only comfortable but also usable. Since it might also involve limits to issues such as structural deflection in beams [2] or footing displacement owing to soil settlement [3] and non-structural issues such as durability [4], cost [5], and other aspects related to stakeholders and operators. The ULS (ultimate limit state) of a structure refers to the maximum design load that causes the structure to collapse [6]. Structural failure occurs due to the loss of the structure's stiffness and strength. However, there are several other limit states that existed before the ULS and structural failure. Designers make use of these other limit states based on the different

*Corresponding author
Email address: moghadas@aut.ac.ir

conditions under which the structure may no longer be able to perform its intended function [7]:

- The serviceability limit state (SLS) [2, 3, 4, 5];
- The ultimate limit state (ULS) [6, 7];
- The fatigue limit state (FLS) [8]; and
- The accidental limit state (ALS) [9].

For a surface to be deemed of good quality, it needs to undergo an appearance inspection, which is a non-destructive testing (NDT) method. This is in accordance with a limit state specified in references [23, 24, 25, and 26]. In this research, a threshold is proposed that can be used to assess the quality of rail surfaces used in industrial settings. This threshold is not only useful for quality control during production but also for inspectors during operation. The limit states are determined by taking into account the proper capacity or strength and are used during the design phase to set a limit for expected structural behavior. They are also used to update the structural state during operation. Since the rail is subjected to cyclic loading, FLS is a crucial factor for railway networks. The threshold will be determined based on this limit state. Meanwhile, the fatigue limit state criterion was employed for the design of pre-stressed concrete sleepers [29, 30].

This study presents an automation tool for preparing an Industrial Information Integration Engineering (IIIE) system. The tool merges machine vision and threshold concepts based on limit states to increase inspection coverage and eliminate errors related to subjective human visual inspection. By maximizing inspection coverage at each turn, a database is prepared and updated with the status of the rail using the IIIE framework. This method enhances the precision of defect growth recognition and quality changes over time in the rail, specifically in detecting the propagation of cracks and estimating fractures. Recent research based on IIIE has also focused on updating the quality status of industrial objects [21, 22].

2. Material and methodology

2.1. Material

The purpose of this study is to investigate the quality of rail as an industrial component in a railway network. For this research, the Tehran subway railway network has been selected as a case study. It spans a length of 253 kilometers and consists of 143 stations, located in both urban and suburban areas of Tehran.

The random checks for this study began in October 2020 and lasted for a year. These checks were conducted at 13 different locations, chosen randomly from eight lines and 26 stations within the network. The maximum velocity allowed on these lines is 80 km/h. Visual head checks were performed on both straight and curved sections of the track. The case study used reinforced concrete for both the sleeper and the track. Additionally, the railway track is situated in tunnels, bridges, and open areas.

2.2. Methodology

To achieve this goal, machine vision techniques that utilize image processing, edge detection, and calculation of the damaged area have been employed to compare it with the alarm threshold. This comparison, integrated within the industrial information framework, results in a perceptron neuron output of either zero or one for each frame. The lighting and camera sync together during data gathering; somehow, any apparent changes on the rail surface, such as cracking and other defects, are detectable by the camera. These defects may affect the performance of the rail and its quality during the operation. In this matter, the setup for capturing images is necessary to be compatible with the environmental conditions while the train is moving. Therefore, the frame rate of the CCD camera has to sync with the lighting frequency and speed of the train. It is necessary to use a softbox in the mainline of the underground tunnel for monitoring the rail surface when artificial light is reflected by the polished rail surface. Therefore, the proposed setup for data gathering is proper for detecting any surface physical damage on the rail as an industrial component. To calculate the area of the damage in the observed parts, edge detection has been applied, and the damaged area is considered for comparison by the maximum hertz ellipsoid contact area between the rail and wheel. Therefore, in each frame, the damaged area has been calculated by its edges and its inside pixels.

Meanwhile, the distance changes between the CCD and the object during the train movement, which affected the scale of the images, were neglected. If the railway track is not smooth and the train has vertical movement, it is possible to scale the rail by comparison with a reference image of the rail.

For better image resolution, a global shot CCD or high frame rate rolling shot CCD should be used. However, frequency lighting provides an economical solution with clear frames. The frame captured from the video in an urban area is as follows:

Figure 1. Frame video capture from head check.

3. Data processing

The database has been prepared from a rail surface status as an object. Machine vision is proposed instead of the traditional visual head check due to operational limitations and obstacles for the visual tests of humans.

3.1. Inspection database

Inspectors evaluate the structural behavior of railway tracks based on their experience. However, machine vision requires setting alarm thresholds. It is important to define the appropriate threshold size for structural defects, such as those found in rails, to ensure sufficient safety. It is also necessary to identify the type of defect before determining the threshold. The International Union of Railways (UIC) has developed guidelines for sustainability and mobility to improve rail transport worldwide. The UIC standard categorizes rail surface irregularities, of which Table 1 lists several important cases [17].

Table 1. Rail Irregularities based on UIC coding.

1- Rail ends 2- Zone away from rail ends	2. Surface of rail head	0. Wear
		1. Surface defects
		2. Shelling
		3. Crushing
		4. Local batter
		5. Wheel burns
		7. Cracking and local subsidence
3- Defects caused by damage to rail	0. Full section	2. Faulty machining
		3. Permanent deformation
4- Welding and resurfacing	2. Thermite welding	1. Transverse
		2. Horizontal or shelling
	7. Resurfacing	1. Transverse
		2. Horizontal or shelling

3.2. Statistical database results

According to the head check results of the mentioned case, the most frequent defects based on the UIC coding system are the surface irregularities with code numbers 227, 127, and 223 (see Figure 2 and Table 1).

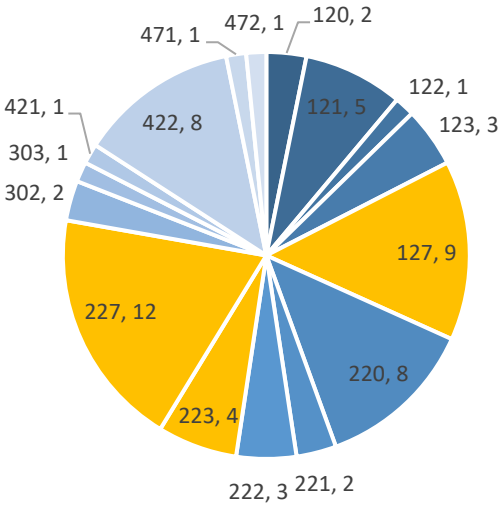

Figure 2. Observed defect in the case study based on UIC-e712 clustering.

Since fatigue-related cracks and crushing are common, machine vision requires specific processing thresholds for this database.

4. Updating alarm thresholds

In the railway track safety system, the stimuli-based alarm model proposes that rail surfaces are monitored, and when some pre-defined threshold based on FLS is violated, the alarm goes off, requesting the decision-maker to act. In other words, the response-based method points out that the inspector defines what constitutes an alarm based on the incoming information and decides whether or not to send the remedial action service to the contractor.

4.1. Fatigue limit state (FLS)

A great deal of scientific effort has been recently conducted on surface irregularities and fatigue, as reviewed by Zhuming et al. [27].

σ_f= Fatigue limit of the unnotched specimen (axial or bending)

σ_{nf}= Fatigue limit of the notched specimen (axial or bending)

$$K_f = \frac{\sigma_f}{\sigma_{nf}} \tag{1}$$

Noting Equation 1, notch is a type of crack simulation and thickness reduction for estimating the fatigue limit. The term K_f is defined as the quotient of the fatigue limit of the smooth specimen to the fatigue limit of a notched specimen and is also labeled as the fatigue strength reduction factor [8]. Peterson and Neuber have described the notch sensitivity factor based on material features [28]. Neuber exploits the average stress along the distance a_N ahead of the notch tip as the effective stress for fatigue limit prediction. In Equation 2, K_t and r_n are the stress concentration factor and notch radius, respectively [8].

$$K_f = 1 + \frac{K_t - 1}{1 + \sqrt{\frac{a_N}{r_n}}} \tag{2}$$

Peterson states that a_P is the point of stress away from the notch tip as the effective stress, based on which the fatigue notch factor K_f can be expressed as in Equation 3 [8].

$$K_f = 1 + \frac{K_t - 1}{1 + \frac{a_P}{r_n}} \tag{3}$$

According to Figure 1, the most common rail irregularity in this research case study is rail contact fatigue (RCF) due to high frequent loads in the subway, according to ongoing observation. RCF on a rail will occur if the stresses exceed a threshold in the contact patch. Surface cracking forms as flakes due to accumulated plastic strain and the pressure and creep forces over time. Therefore, the failure mechanism due to wheel rotation on the rail surface is RCF, intensified by surface fatigue cracks on the rail. A model for the prediction of rolling contact fatigue (RCF) has been developed by Ekberg et al. [11, 12], and an index called FI_{surf} has been developed for this purpose [10, 18], Equations 4 and 5.

$$FI_{surf} = \frac{|F_t|}{N} - \frac{2\pi abk}{3N} = \mu - \frac{2\pi abk}{3N} \tag{4}$$

$$\mu = \frac{|F_t|}{N} = \frac{\sqrt{F_x^2 + F_y^2}}{N} \tag{5}$$

In these equations, μ is the utilized friction coefficient, F_x and F_y are lateral loads in the rail and wheel axle directions. Moreover, N is the normal contact force, F_t is the lateral contact force, a and b are half the Hertz contact ellipse diameter, and k is the yield limit in pure shear (torsion). Accordingly, RCF occurs if the value for this index is greater than zero (FI_{Surf} >0).

Based on recent models, the area of cracks and notches is important for failure due to fatigue and RCF when a and b have been changed and have effects on the Hertz contact ellipse. Therefore, the proposed method in this research focuses on damaged area estimation by mechanized visual inspection and machine learning for clustering defects based on alarm thresholds and crack area estimation.

4.2. Hertz contact ellipse

The zone of interaction of two curved surfaces of the rail and wheel in contact is ideally zero; therefore, this will cause infinite stress and instant failure of the rail. However, based on surface stiffness changes due to railhead irregularities and during the application of load, a real area of contact is formed. Thus, the form of the contact area depends on the materials of the rail and the load. The German physicist Heinrich Hertz (1881) first studied this stress, and, in his honor, the name of stress in this contact area was given as Hertzian stress [16]. The Hertzian stress and deformation in this contact area have been plotted in a recent study and finite element model in Figure 3.

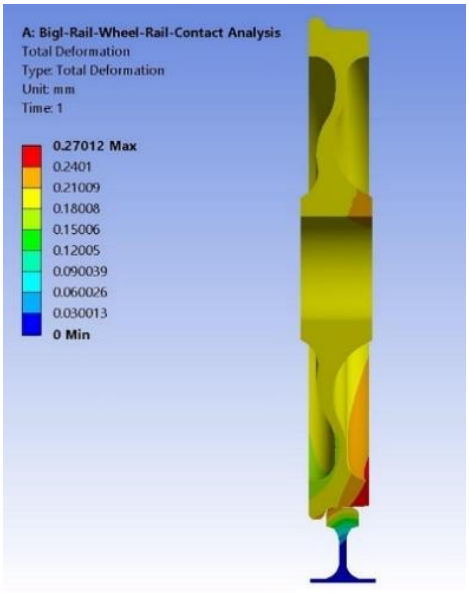

Figure 3. Deformation plot of Big Rail Wheel (cross-section view) [15].

Based on this model, the maximum deformation will occur on the railhead and gauge corner, and RCF also appears in the same zone as the railhead. This defect is also more common in the inner rail of the curves.

4.3. Machine learning and damage detection method

Recently, neural networks have been exploited to solve problems such as detection and classification by activation functions. Time series data and state comparisons based on the limit state in each turn have a reward as an index. Meanwhile, if the volume of irregularities is greater than the threshold, the alarms will be active.

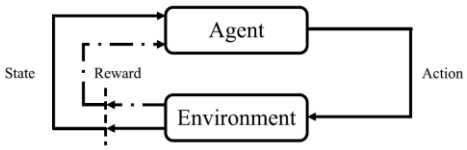

Figure 4. Agent environment interaction [13].

This paper suggests a relative computational algorithm based on neural networks for the establishment of alarm thresholds for railway engineering structures to indicate when contingency actions are needed to improve safety. On this occasion, the assessment of the structure has been done by a neural network based on perceptron neurons. The result is that the critical points in railway networks in terms of safety are detectable by a camera as an agent. In this matter, estimating the damaged area on the rail surface prepares the environment, and the perceptron neuron will check the volume of the damaged area. Based on Figure 6, if the damaged area is higher than the fatigue threshold, the alarm goes off. If the damaged area is lower than the expected threshold, the reward will be 0, and for the higher amount, the reward will be 1.

5. Results

5.1. Threshold estimation

In this case, based on the flowchart in Figure 5 (Result 2), the threshold estimation has been calculated for the case study. Therefore, the rail specifications for FLS and FI calculations are as follows:

According to Equation 6 [19], the yield stress in shear (K) has been estimated at 346.987 MPa.

$$K = \frac{\sigma_y}{\sqrt{3}} \qquad (6)$$

In the Tehran subway, the train axle load is different for urban and suburban areas. In this case study, the urban area has been considered for this research. Meanwhile, the axle load for the train (AC Series 100) is 9.5 tons. The friction coefficient for both steel surfaces will be between 0.1 and 0.2 for uneven surfaces. Additionally, other parameters have been suggested as follows:

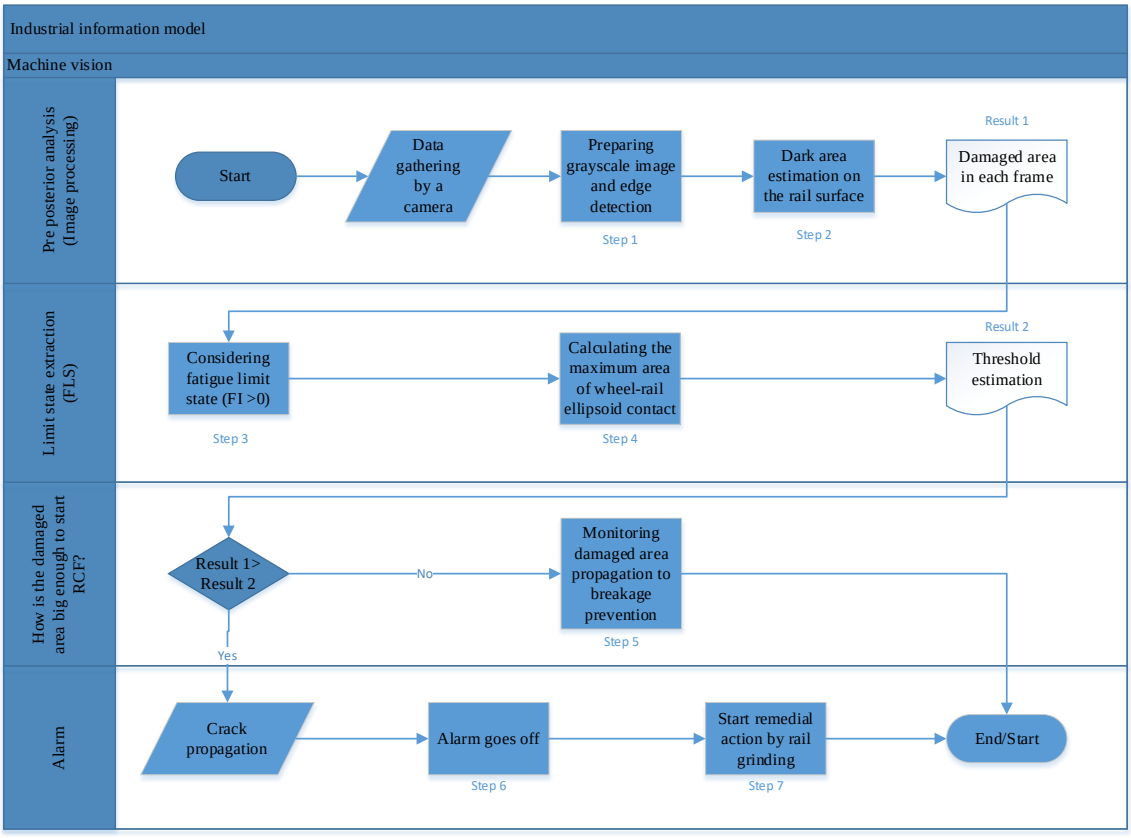

Figure 5. Damage analysis process.

Table 2. Test result for finding proof offset (σ_y).

No	Diameter D (mm^2)	Initial cross-section area $S_0(mm^2)$	Proof offset 0.2% R_t Mpa	Ultimate strength R_t Mpa	Relative elongation %A $L_e = 5.65\sqrt{S_s}$	Cross-section area reduction %Z
1	9.96	77.91	598	1011	11.5	22
2	9.91	77.13	604	997	12.5	23

$\mu = 0.2$

$N = 9.5\ t = 9500\ kg$

$K = 346.987\ MPa = 3538.288\ kg/cm^2$

$$FI>0 => \mu - \frac{2\pi abk}{3N} > 0$$

$$=> \frac{\mu * 3N}{2k} > \pi ab \quad (7)$$

πab is the ellipsoid area between the wheel and rail contact zones. Based on Equation 7, it is necessary to limit this area to less than 0.0805 $\boldsymbol{mm^2}$ if RCF is undesirable on the rail surface. The cracks and damaged areas have to be lower than this contact area. In other words, the maximum damaged area has to be lower than this threshold.

5.2. Damaged area estimation

The damaged area has been estimated in videos and shown in Figure 6. In Figure 6, the damaged area has been shown.

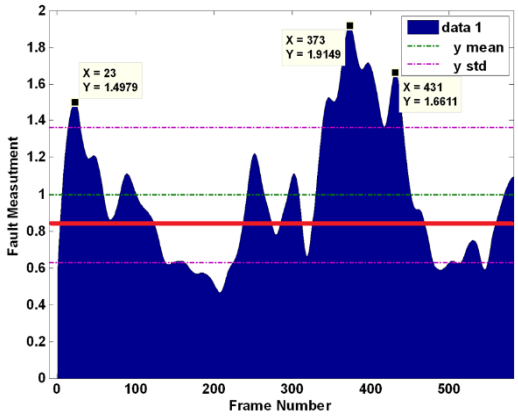

Figure 6. Threshold and damaged area comparison.

6. Conclusion

The results show that the Hertz contact ellipse's area between the rail and wheel is (πab) $0.805Cm^2$. Based on BS EN 13674-1, the rail head width is 70 mm, and the damaged area will reduce the width of the wheel and rail contact area. To detect surface defects on the rail and measure the rate of irregularity growth over time, it is necessary to establish thresholds for machine vision instead of relying on visual tests. Therefore, it is necessary to ensure that the damaged area in each frame of the video is lower than the threshold. With this neural network after edge detection and damaged area estimation, the volume of the damaged area will be compared with the threshold, and for a higher quantity, the RCF is probable and the alarm goes off.

Data analysis for damage detection after automation is comparable over time based on indexes. However, traditional visual rail head checks lack quantitativeness. The quality of the material source can be determined by the rate of damage growth. This information can also aid in the management of maintenance and improve the efficiency of maintenance activities

Declaration of Conflicting Interests

The authors declare no conflict of interest.

Acknowledgements

I would like to express my very great appreciation to Mr. Saed Nadery for his valuable suggestions during the development of this research work. His willingness to give his time so generously has been very much appreciated. Finally, I wish to thank my parents and my wife for their support and encouragement throughout my study.

References

[1] Basteskår, M., Engen, M., Kanstad, T., Johansen, H., & Fosså, K. T. (2019). Serviceability limit state design of large concrete structures: Impact on reinforcement amounts and consequences of design code ambiguity. Engineering Structures, 201(October), 109816. https://doi.org/10.1016/j.engstruct.2019.109816

[2] Honfi, D., Mårtensson, A., & Thelandersson, S. (2012). Reliability of beams according to Eurocodes in serviceability limit state. Engineering Structures, 35, 48–54.

[3] Huffman, J. C., Strahler, A. W., & Stuedlein, A. W. (2015). Reliability-based serviceability limit state design for immediate settlement of spread footings on clay. Soils and Foundations, 55(4), 798–812.

[4] Amadio, C., Fragiacomo, M., & MacOrini, L. (2012). Evaluation of the deflection of steel-concrete composite beams at serviceability limit state. Journal of Constructional Steel Research, 73, 95–104.

[5] Rhee, S. J., & Ishii, K. (2003). Using cost based FMEA to enhance reliability and serviceability. Advanced Engineering Informatics, 17(3–4), 179–188.

[6] Kuznecovs, A., Ringsberg, J. W., Johnson, E., & Yamada, Y. (2020). Ultimate limit state analysis of a double-hull tanker subjected to biaxial bending in intact and collision-damaged conditions. Ocean Engineering, 209(March), 107519.

[7] Paik, J. K. (2018). Ultimate Limit State Analysis and Design of Plated Structures. Wiley & Sons.

[8] Liu, Y., Deng, C., Gong, B., He, Y., & Wang, D. (2021). Fatigue limit prediction of notched plates using the zero-point effective notch stress method. International Journal of Fatigue, 151(April), 106392.

[9] Benassai, G., Campanile, A., Piscopo, V., & Scamardella, A. (2014). Ultimate and accidental limit state design for mooring systems of floating offshore wind turbines. Ocean Engineering, 92, 64–74.

[10] E. Kassa & J. C. O. Nielsen (2008) Stochastic analysis of dynamic interaction between train and railway turnout, Vehicle System Dynamics: International Journal of Vehicle Mechanics and Mobility, 46:5, 429-449, DOI: 10.1080/00423110701452829

[11] Ekberg, A., Kabo, E. and Andersson, H., 2002, An engineering model for prediction of rolling contact fatigue of railway wheels. Fatigue and Fracture of Engineering Materials and Structures, 25, 899–909. DOI: 10.1046/j.1460-2695.2002.00535.x

[12] Ekberg, A. and Stokoszki, P. (2001) Anisotropy and fatigue of railway wheels. International Journal of Fatigue, 23, 29-43. DOI: 10.1016/s0142-1123(00)00070-0

[13] Fink, O., Wang, Q., Svensén, M., Dersin, P., Lee, W. J., & Ducoffe, M. (2020). Potential, challenges and future directions for deep learning in prognostics and health management applications. Engineering Applications of Artificial Intelligence, 92(January), 103678. https://doi.org/10.1016/j.engappai.2020.103678

[14] Grassie, S. L. (2012). Rail irregularities, corrugation and acoustic roughness : characteristics , significance and effects of reprofiling. Journal of rail and rapid transit, 226(5),542–557.

[15] Gupta, A., Pradhan, S. K., Bajpai, L., & Jain, V. (2020). Numerical simulation of contact behavior between rail wheel and rails of a new road cum rail vehicle. Materials Today: Proceedings, 46, 3966–3974.

[16] Knothe, K. (2008). History of wheel/rail contact mechanics: From Redtenbacher to Kalker. Vehicle System Dynamics, 46(1–2), 9–26.

[17] International union of railway. (2002). UIC code 712- Rail defects (4th edition).

[18] Ekberg, A., Kabo, E., & Andersson, H. (2001). PREDICTING ROLLING CONTACT FATIGUE OF RAILWAY WHEELS, 1–7.

[19] Doyle, N. F. (1980). Railway Track Design: A Review of Current Practice Occasional Paper. BUREAU OF TRANSPORT ECONOMICS BHP Melbourne Research Laboratories, 303.

[20] ISO 6892-1:2016. (2016). Metallic materials tensile test (Vol. 1).

[21] Li, Z., & Burgueño, R. (2019). Structural information integration for predicting damages in bridges. Journal of Industrial Information Integration, 15(November 2018), 174–182. https://doi.org/10.1016/j.jii.2018.11.004

[22] Li, N., Zhao, L., Bao, C., Gong, G., Song, X., & Tian, C. (2021). A real-time information integration framework for multidisciplinary coupling of complex aircrafts: an application of IIIE. Journal of Industrial Information Integration, 22(February).

[23] Zhao, D., Xue, D., Wang, X., & Du, F. (2021). Adaptive vision inspection for multi-type electronic products based on prior knowledge. Journal of Industrial Information Integration, (September), 100283. https://doi.org/10.1016/j.jii.2021.100283

[24] Zhang, Z., Liang, M., & Liu, Z. (2021). A novel decomposition model for visual rail surface inspection. Electronics (Switzerland), 10(11), 1–20. https://doi.org/10.3390/electronics10111271

[25] Xu, P., Zhu, C. L., Zeng, H. M., & Wang, P. (2020). Rail crack detection and evaluation at high speed based on differential ECT system. Measurement: Journal of the International Measurement Confederation, 166, 108152. https://doi.org/10.1016/j.measurement.2020.108152

[26] Wang, K., Hao, Q., Zhang, X., Tang, Z., Wang, Y., & Shen, Y. (2020). Blind source extraction of acoustic emission signals for rail cracks based on ensemble empirical mode decomposition and constrained independent component analysis. Measurement: Journal of the International Measurement Confederation, 157,107653.https://doi.org/10.1016/j.measurement.2020.107653

[27] WALTER D. PILKEY, DEBORAH F. PILKEY, Z. B. (2020). Peterson's stress concentration factors. John Wiley & Sons, Inc. Retrieved.

[28] Zehsaz, M., Hassanifard, S., & Esmaeili, F. (2010). Fatigue life estimation for different notched specimens based on the volumetric approach. EPJ Web of Conferences, 6, 1–10. https://doi.org/10.1051/epjconf/20100642001.

[29] Li, Dan, Sakdirat Kaewunruen, Ruilin You, and Ping Liu. "Fatigue life modelling of railway prestressed concrete sleepers." In Structures, vol. 41, pp. 643-656. Elsevier, 2022.

[30] You, Ruilin, and Sakdirat Kaewunruen. "Evaluation of remaining fatigue life of concrete sleeper based on field loading conditions." Engineering Failure Analysis 105 (2019): 70-86.